Manipulating Growth and Propagation of Correlations in Dipolar Multilayers: From Pair Production to Bosonic Kitaev Models

Thomas Bilitewski[1] and Ana Maria Rey[2,3]
[1]Department of Physics, Oklahoma State University, Stillwater, Oklahoma 74078, USA
[2]JILA, National Institute of Standards and Technology and Department of Physics, University of Colorado, Boulder, Colorado 80309, USA
[3]Center for Theory of Quantum Matter, University of Colorado, Boulder, Colorado 80309, USA

(Received 22 November 2022; accepted 14 July 2023; published 3 August 2023)

We study the nonequilibrium dynamics of dipoles confined in multiple stacked two-dimensional layers realizing a long-range interacting quantum spin 1/2 XXX model. We demonstrate that strong in-plane interactions can protect a manifold of collective layer dynamics. This then allows us to map the many-body spin dynamics to bosonic models. In a bilayer configuration we show how to engineer the paradigmatic two-mode squeezing Hamiltonian known from quantum optics, resulting in exponential production of entangled pairs and generation of metrologically useful entanglement from initially prepared product states. In multilayer configurations we engineer a bosonic variant of the Kitaev model displaying chiral propagation along the layer direction. Our study illustrates how the control over interactions, lattice geometry, and state preparation in interacting dipolar systems uniquely afforded by AMO platforms such as Rydberg and magnetic atoms, polar molecules, or trapped ions allows for the control over the temporal and spatial propagation of correlations for applications in quantum sensing and quantum simulation.

DOI: 10.1103/PhysRevLett.131.053001

The individual particle control offered by quantum gas microscopes [1] and optical tweezers [2], and the impressive advances in spectroscopic methods [3] complemented by the capability of experiments to trap and manipulate a broad range of atomic, molecular, and optical systems featuring diverse types of interactions (from contact [4,5] to dipolar [6–13] to all-to-all [14–19]) are opening untapped opportunities for quantum simulation [20–22], metrology [23], and computation [24–26]. In these systems it is now possible to explore the propagation and growth of quantum entanglement and correlations [27], which is crucial for demonstrating their quantum advantage.

One of the most basic mechanisms for entanglement growth, which is also at the very heart of foundational questions in quantum mechanics [28,29], is the creation of entangled states consisting of pairs of correlated particles in the guise of two-mode squeezed (TMS) states [30–32]. These states were originally understood in quantum optics in the context of parametric amplification, but have been shown to be relevant to a wide range of phenomena including the Schwinger effect in high energy physics [33,34], the Unruh thermal radiation in general relativity [35], mode-changing collisions in spinor condensates [36–39], and thermofield double states in the holographic correspondence relating a quantum-field theory to a gravitational theory in one higher dimension [40,41].

In this Letter, we explore various ways to produce correlated pairs during the nonequilibrium many-body dynamics of long-range interacting spin-1/2 arrays, realizable in polar molecules [6–8], magnetic atoms [42], or Rydberg arrays [43–46], prepared in a stack of two-dimensional layers. Across these platforms single-site [47], as well as layer selective control and state preparation [48], and high filling fractions in tweezer arrays [45,46,49] have been demonstrated. Here, we use strong in-plane Heisenberg interactions to lock the spin of each layer into a collective spin, with magnitude set by the number of particles in each layer, and show that by preparing different initial orientations of the collective spins (enabled by layer-selectivity), interlayer interactions [48] can be used to engineer distinct types of pair production processes.

One of them is the paradigmatic two-mode squeezing Hamiltonian [30–32] known for its capability to generate metrologically useful states. Originally encapsulated by the Einstein, Podolsky, and Rosen (EPR) paradox [28,29], two-mode squeezing occurs when two separate ensembles A and B are correlated such that the relative fluctuations between the sum and difference of two quadratures can be determined below the Heisenberg uncertainty constraint [50]. In this work A and B are bosonic excitations in different spatially separated layers generated exponentially fast through long-range dipolar interactions between the particles allowing fast scalable entanglement generation in large systems. Pioneering work on spatially distributed entanglement has been accomplished using atom-light interactions in photonic systems [51–53], and hot atomic vapors [54,55], as well as in Bose-Einstein

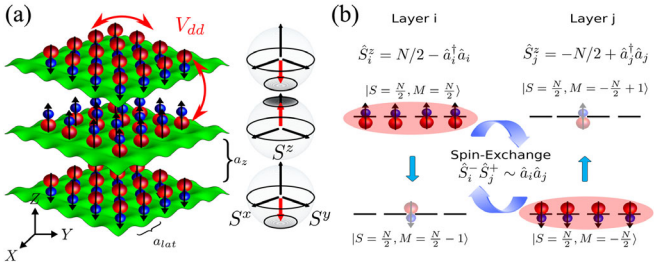

FIG. 1. Illustration of spin 1/2 dipoles in multilayers and mapping to bosonic pair creation. (a) Dipoles in stacked 2D layers of a 3D optical lattice are prepared layer selectively in (distinct) coherent spin states illustrated by the Bloch spheres. They interact via long-range (dipolar) interactions within and between layers. (b) Strong in-plane interactions $\hat{S}_i \cdot \hat{S}_i$ (illustrated as red ellipse) couple spins within a layer resulting in collective behavior. Interlayer dipolar spin exchange $(\hat{S}_i^+ \hat{S}_j^-)$ maps to pair creation of bosonic collective excitations.

condensates [56,57], and more generally in quantum networks [58–62]. However, the possibility of using long-range interactions to directly correlate spatially separated arrays without the detrimental degradation of coherence from motional effects or photon loss can offer significant opportunities for quantum metrology, in particular in terms of scalability and speed of entanglement generation.

Furthermore, by preparing an initial state with states cyclically staggered along three perpendicular Bloch vector directions we show it is possible to engineer a bosonic variety of the Kitaev model [63] which shows remarkable properties such as phase-dependent chirality, drastic sensitivity to boundary conditions and rich dynamical behaviors [64]. While there have been proposals to generate bosonic Kitaev models in coupled cavities subject to parametric driving [64], their implementation in long lived molecular or atomic states interacting via long range interactions can offer important advantages for their preparation, detection and storage.

Model.—We consider spins interacting via long-range interactions in two or more two-dimensional layers as shown in Fig. 1(a), prepared, for example, via a deep 3D optical lattice. We assume distinct in-plane lattice spacing a_{lat} and layer spacing a_Z. We restrict dynamics to two internal states representing a spin 1/2 degree of freedom with dynamics determined by the XXX Hamiltonian

$$\hat{H}_{\mathrm{XXZ}} = 1/2 \sum_{\mathbf{i}\neq\mathbf{j}} V_{\mathbf{ij}} \left[\frac{1}{2} (\hat{s}_{\mathbf{i}}^+ \hat{s}_{\mathbf{j}}^- + \hat{s}_{\mathbf{i}}^- \hat{s}_{\mathbf{j}}^+) + \hat{s}_{\mathbf{i}}^z \hat{s}_{\mathbf{j}}^z \right], \quad (1)$$

where $\mathbf{i}$, $\mathbf{j}$ are three-dimensional positions (i_X, i_Y, i_Z) and i_X, i_Y run along the positions in a given two-dimensional layer of size $L \times L$ indexed by i_Z. The spin operators $\hat{s}_{\mathbf{i}}^\alpha = \hat{\sigma}_{\mathbf{i}}^\alpha/2$ are given in terms of the Pauli matrices $\hat{\sigma}^{x,y,z}$ that act on the spin at site $\mathbf{i}$. For specificity we consider dipolar interactions of the form $V_{\mathbf{ij}} = V_{dd}(\mathbf{r_i} - \mathbf{r_j})$ with $V_{dd}(\mathbf{r}) = (C_{dd}/r^3)(1 - 3\hat{Z}^2)$ parametrized by a dipolar coupling strength C_{dd}. The Hamiltonian contains both intralayer as well as interlayer Heisenberg interactions, the relative strength of which can be tuned by changing the ratio a_Z/a_{lat}.

We consider initial states for which all spins in a layer i are prepared in the same state and form a fully polarized state with the collective spin $\vec{S}_i = \sum_{i_X,i_Y} \vec{s}_{i_X,i_Y,i}$ pointing in a layer-dependent direction $\langle \vec{S}_i \rangle = N/2 \vec{n}_i$, where $N = L^2$ at unit filling, as illustrated for alternating anti-aligned layer spins $\vec{n}_i = (-1)^i \hat{z}$ in Fig. 1(a). Any such state is an eigenstate of the intralayer interactions, and, thus, of the full Hamiltonian in the large layer separation limit. The capability to layer-selectively prepare and control such states has been experimentally demonstrated [48].

The intralayer interactions then reduce to $V_{i,i}^{\mathrm{av}} \vec{S}_i \cdot \vec{S}_i$, with the layer-averaged interactions $V_{ij}^{\mathrm{av}} = 1/N^2 \sum_{i_X,i_Y,j_X,j_Y} V_{(i_X,i_Y,i),(j_X,j_Y,j)}$. This $\vec{S}_i \cdot \vec{S}_i$ term creates an energy cost for states with $\langle \vec{S}_i^2 \rangle < N/2(N/2+1)$ compared to permutationally symmetric states of maximal spin-length $\langle \vec{S}_i^2 \rangle = N/2(N/2+1)$, suppressing transitions out of the collective manifold [65–69]. We emphasize that the specific spatial dependence of the interactions is not material at short times as long as intraplane versus interplane interactions are tunable. At later times the spatial range of the interactions and the geometry will dictate the timescale for which the collective state assumption remains valid.

Within the collective manifold the dynamics is described by

$$\hat{H}_{\mathrm{layer}} = 1/2 \sum_{i\neq j} V_{ij}^{\mathrm{av}} \left[\frac{1}{2} (\hat{S}_i^+ \hat{S}_j^- + \mathrm{H.c.}) + \hat{S}_i^z \hat{S}_j^z \right], \quad (2)$$

where we have omitted the constant contribution from the in-plane interactions in the fully symmetric manifold. The natural scale for the time evolution is set by the layer-averaged interlayer interaction, which for convenience we define as $V = V_{i,i+1}^{\mathrm{av}}$.

Bilayer.—We first study the case of a bilayer configuration with initially antialigned layer spins, $\langle \vec{S}_1(t=0) \rangle = -\langle \vec{S}_0(t=0) \rangle = N/2\hat{z}$, as shown in Fig. 1(b).

We simulate the quantum dynamics of the full dipolar spin model using the discrete truncated Wigner approximation (dTWA) [70–75]. In the inset of Fig. 2 we show the time evolution of the total layer spin length $\langle \hat{S}_i^2 \rangle$ for a range of layer spacings a_Z/a_{lat}. While for closely spaced layers the dynamics quickly leaves the fully collective manifold resulting in rapid decay, for sufficiently large spacings we observe a transition to robust collective behavior with the spin-length remaining maximal throughout the dynamics. This is readily explained by the relative increase of the in-plane interactions, which gap protect the permutationally symmetric manifold in each layer, compared to the

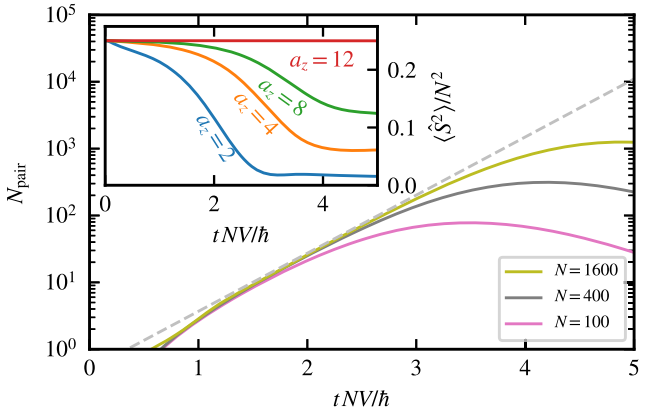

FIG. 2. Exponential pair-creation and dynamical phase transition (DPT) in a dipolar bilayer. Main panel: Exponential growth of bosonic excitations, $N_{\rm pair} = N - S_1^z + S_0^z$, versus time compared to the two-mode squeezing prediction $N_{\rm pair} = 2\sinh^2(SVt/\hbar)$ (gray dashed). Bilayer with $a_Z/a_{\rm lat} = 12$ in an initially antialigned spin state, $S_1^z(0) = -S_0^z(0) = N/2$ with $L = 10$, 20, 40 ($N = 100$, 400, 1600 per layer). Inset: DPT to collective regime. Spin-length $\langle \hat{S}^2 \rangle / N^2$ versus time for different layer spacings $a_Z/a_{\rm lat} = 2$, 4, 8, 12 displaying the transition to collective behavior for $L = 40$ ($N = 1600$).

interplane interactions, which allow excitations out of this manifold, with increasing layer distance.

As a first result we thus observe that for an appropriate ratio of a_Z/a_{lat} (or generically for sufficiently strong intraplane and sufficiently homogeneous interlayer interactions) the dynamics of the full model indeed closely follows the collective model, allowing the simulation of 1D Heisenberg chains with large (tunable) spin.

Mapping to two-mode squeezing.—Exploiting the collectiveness of the dynamics, we use a standard Holstein-Primakoff (HP) transformation [76] as $S_1^z = S - \hat{a}^\dagger a$, $S_1^+ = \sqrt{2S}\sqrt{1 - (\hat{a}^\dagger \hat{a}/2S)}\hat{a}$, $S_1^- = (S_1^+)^\dagger$, and $S_0^z = -S + \hat{b}^\dagger b$, $S_0^+ = \sqrt{2S}\hat{b}^\dagger\sqrt{1 - (\hat{b}^\dagger\hat{b}/2S)}$, $S_0^- = (S_0^+)^\dagger$ with $S = N/2$ and $\hat{a}$ and $\hat{b}$ bosonic operators. To quadratic order in the $\hat{a}$ and $\hat{b}$ operators we obtain

$$H_{\rm pair} = SV((\hat{a}^\dagger\hat{b}^\dagger + \hat{a}\,\hat{b}) + (\hat{a}^\dagger\hat{a} + \hat{b}^\dagger\hat{b})), \qquad (3)$$

where $S_0^+S_1^- + S_0^-S_1^+$ maps to pair creation $2S(\hat{a}^\dagger\hat{b}^\dagger + \hat{a}\,\hat{b})$, while $S_0^zS_1^z$ maps to $-S^2 + S(\hat{a}^\dagger\hat{a} + \hat{b}^\dagger\hat{b})$. To cancel this Ising induced term we apply an additional staggered field $\sum_i (-1)^i h S_i^z$ with $h = -SV$ obtaining the pure two-mode squeezing Hamiltonian. Then, the dynamics corresponds to the resonant creation of correlated pairs of bosonic excitations in both layers. This mapping and the pair creation due to dipolar interlayer spin exchange in the collective spin manifold is illustrated in Fig. 1(b).

Exponential pair creation.—A first prediction of this mapping is the exponential creation of bosonic pairs of excitations $N_{\rm pair} = (\hat{a}^\dagger\hat{a} + \hat{b}^\dagger\hat{b}) = N - S_1^z + S_0^z$ as $N_{\rm pair}(t) = 2\sinh^2(SVt/\hbar)$ [30–32]. In Fig. 2 we demonstrate that the dynamics of the full dipolar bilayer based on dTWA simulations also shows exponential creation of pairs. In fact, it closely follows the prediction of the two-mode squeezing Hamiltonian (dashed gray line) as long as $N_{\rm pair} \lesssim 0.1N$, beyond which the Holstein-Primakoff approximation is invalid, and higher order corrections become relevant [77]. This exponential creation can be directly observed in experiment by measuring the population difference $S_1^z - S_0^z$ between the layers.

Squeezed quadratures.—Because of the correlated creation of pairs in two modes, the Hamiltonian [Eq. (3)] generates squeezed states in hybrid quadratures [30–32]. Translating these well-known results from the bosonic operators into our original spin operators we find that $S_0^x + S_1^y$ and $S_0^y - S_1^x$ correspond to squeezed quadratures, and $S_0^x - S_1^y$ and $S_0^y + S_1^x$ correspond to the antisqueezed quadratures. Consequently, the variance of these hybrid operators is predicted to evolve as $\mathrm{Var}[\mathcal{O}_\pm] = N/2e^{\pm 2SVt/\hbar}$, where we use $\pm$ to refer to the antisqueezed or squeezed quadratures. Measuring this variance and observing the squeezing requires measuring spin correlators between the layers of the form $S_0^\alpha S_1^\beta$, which via layer-selective pulses these can be reduced to measurements of $S_0^zS_1^z$, or, equivalently, population correlations between the layers.

Based on the full dynamics of the dipolar bilayer we confirm this prediction in Fig. 3, which shows the exponential decrease of the variance of the squeezed quadratures for a range of layer spacings (antisqueezed quadratures not shown behave accordingly). We observe that the minimal squeezing achievable relies on a sufficiently large layer separation to ensure we stay in the fully collective

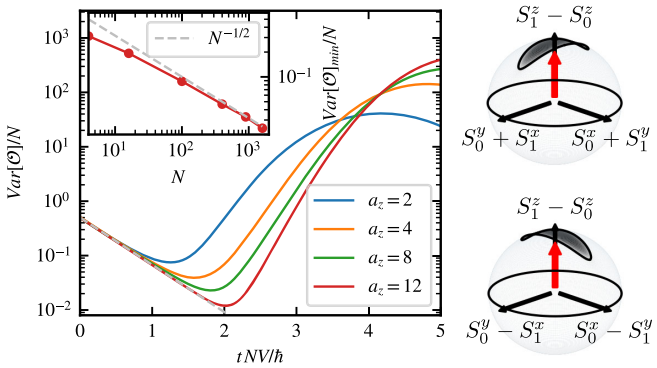

FIG. 3. Exponential two-mode squeezing. Main panel: Time evolution of the squeezed variances for different layer spacings, compared to the two-mode-squeezing prediction $\mathrm{Var}[\mathcal{O}] = N/2e^{\pm 2SVt/\hbar}$ (gray dashed) for $L = 40$ ($N = 1600$ per layer). Bloch spheres using the appropriate combinations of the layer-spin operators illustrating squeezed and antisqueezed variances. Inset: N dependence of the minimal variance achieved ($a_Z/a_{\rm lat} = 12$) demonstrating $N^{-1/2}$-scaling (gray dashed).

manifold. If that is the case, we observe excellent agreement up to a time at which $N_{\text{pair}} \sim \sqrt{N}$, where corrections to the quadratic Hamiltonian become relevant [77]. As a consequence, the minimal achievable squeezing scales as $N^{-1/2}$ with respect to the total number of spins as shown in the inset of Fig. 3. These generated states directly allow quantum-enhanced sensing using recently devised Ramsey protocols only requiring measurements of the collective spin variables and collective spin rotations of the individual layers [78]. We also find the squeezing to be robust to finite filling of the lattices [77]. This is an important observation since only tweezers arrays have demonstrated the capability to operate at unit filling [49], while current optical lattice setups are still limited to operate at moderate filling fraction [47].

Bosonic Kitaev model and chiral spin transport.—We next extend our discussion to multiple layers, and exploit the capability to prepare more complex initial states. We consider a noncoplanar spiral state where we take the layer spin directions to be $\vec{n}_i = \hat{x}$, $\hat{y}$, and $\hat{z}$ in order and repeating periodically along the layers [Fig. 4(a)].

We then rotate the local spin basis in each layer to be aligned with the initially prepared spin direction via $S_j = U_j^\dagger \tilde{S}_j U_j$ with $U_j = e^{ij2\pi/3(\hat{S}_j^x+\hat{S}_j^y+\hat{S}_j^z)/\sqrt{3}}$. In this rotated frame, the XXX Hamiltonian can be projected onto the fully symmetric state in each layer. If we also restrict the interactions to nearest-layer interactions, it can be mapped to

$$\hat{H} = V\sum_i (U_i^\dagger \tilde{S}_i U_i)\cdot(U_j^\dagger \tilde{S}_j U_j) \tag{4}$$

$$= V\sum_i (\tilde{S}_i^x \tilde{S}_{i+1}^z + \tilde{S}_i^y \tilde{S}_{i+1}^x + \tilde{S}_i^z \tilde{S}_{i+1}^y). \tag{5}$$

We then perform a unitary transformation to remove a global rotation of all spins via $U(t) = e^{-itV/\hbar\sum_i (\hat{S}_i^x+\hat{S}_i^y+\hat{S}_i^z)}$, and finally use a Holstein-Primakoff transformation ([77]) to obtain up to quadratic order

$$\hat{H} \approx SV\sum_j (i\hat{a}_j\hat{a}_{j+1}^\dagger - i\hat{a}_j^\dagger\hat{a}_{j+1}^\dagger + \text{H.c.}), \tag{6}$$

where $\hat{a}_j$ is a bosonic creation operator acting on the time and layer-dependent vacuum state. This Hamiltonian is the bosonic version of the famous Kitaev model first introduced in Ref. [64]. It can be expressed in terms of Hermitian quadrature operators, $\hat{x}_j = (\hat{a}_j + \hat{a}_j^\dagger)/\sqrt{2}$, $\hat{p}_j^\dagger = (\hat{a}_j - \hat{a}_j^\dagger)/(i\sqrt{2})$ as $\hat{H} = -2SV\sum_j \hat{p}_j\hat{x}_{j+1}$, whose equations of motion are fully decoupled $\dot{\hat{x}}_i = -2SV/\hbar\hat{x}_{i+1}$, and $\dot{\hat{p}}_i = 2SV/\hbar\hat{p}_{i-1}$, and therefore show perfect chiral transport: the $\hat{x}$ quadratures are only coupled to $\hat{x}$ quadratures to the right and the $\hat{p}$ quadratures are only coupled to $\hat{p}$ quadratures to the left.

We can observe the chiral nature of the excitations in the dynamics of the spin operators. To gain some intuition we first consider the evolution of the spin-operators which perturbatively evolve as $\hat{S}_i^\alpha(t) \approx \hat{S}_i^\alpha + (it/\hbar)[H, \hat{S}_i^\alpha] = \hat{S}_i^\alpha + (iVt/\hbar)\epsilon^{\gamma\alpha\beta}(\hat{S}_{i-1}^\gamma + \hat{S}_{i+1}^\gamma)\hat{S}_i^\beta$. For a site i initially pointing along z, this reduces to $\hat{S}_i^\alpha(t) \approx \hat{S}_i^\alpha + (iVt/\hbar)(\epsilon^{y\alpha z}\hat{S}_{i-1}^y + \epsilon^{x\alpha z}\hat{S}_{i+1}^x)\hat{S}_i^z$. Thus, we see that the x component at site i couples to the y component at site $i-1$, and the y component at site i couples to the x component at site $i+1$. This behavior, when understood in the properly rotated initial frame introduced above, maps to y quadratures only coupling to y quadratures to the right, and x quadratures only coupling to x quadratures to the left, featuring the anticipated chiral behavior.

For the full dipolar spin dynamics there is not a simple global unitary transformation to eliminate the mean field dynamics. Therefore, to cleanly observe the chiral response we require a frame-independent quantity. This can be achieved by computing the spin Green's function, defined as $G_{ij}^{\alpha\beta}(t) = i\langle[S_i^\alpha(t=0), S_j^\beta(t)]\rangle$ that measures the effect of a perturbation in spin component α at $t=0$ on the time-evolved operator along spin-component β at site j and time t. Its singular values measure the strength of response and the components of the left eigenvectors provide information about the spin projection that generated the response. Both are insensitive to the global spin orientation

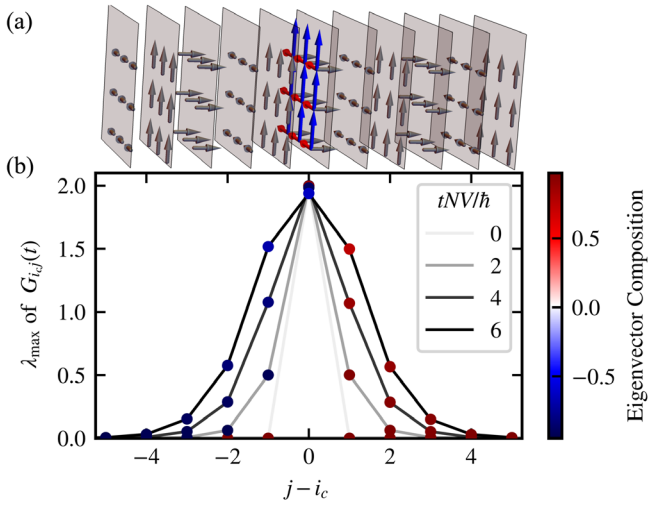

FIG. 4. Chirality of spin transport in a multi-layer system of dipoles. (a) Layers are prepared in a noncoplanar spiral state with the collective layer spin pointing along $\hat{x}, \hat{y}, \hat{z}$ repeating periodically (gray arrows). The central layer also shows the local x (red, into plane) and y (blue) direction. (b) Largest singular value $\lambda_{\max}$ (measuring the strength of the chiral response to a perturbation) of the spin Green's function $G_{i_c,j}^{\alpha\beta}(t) = i\langle[S_{i_c}^\alpha(t=0), S_j^\beta(t)]\rangle$ at fixed times as indicated in the legend versus distance j. Color bar ($|v^x|^2 - |v^y|^2$) indicates the direction of the corresponding left eigenvector $\mathbf{v}$ showing the spin direction of the perturbation that induced the chiral dynamics. System with $L = 10$ ($N = 100$ molecules per layer) with 12 total layers.

generated by the MF dynamics. In Fig. 4(b) we show the largest singular value (measuring the strength of response) as a function of distance from the central layer i_c (which initially points along z). The color scale shows the spin direction of the corresponding left eigenvector which is pointing (almost) purely along x (red) to the right ($j > i_c$), while it is (almost) purely along y (blue) to the left ($j < i_c$). Thus, correlations that propagate to the right originate from $S^x_{i_c}(t=0)$, while correlations that propagate to the left originate from $S^y_{i_c}(t=0)$, demonstrating genuine chiral behavior. We also compare the full dipolar spin model to the analytical solution of the bosonic model and observe good quantitative agreement between both solutions up to times where boundary effects become relevant [77].

Outlook.—In summary, our work demonstrates the large space of opportunities, uniquely enabled by the capability to spatially select, prepare, and measure quantum states, to study novel nonequilibrium phenomena and to control the growth and propagation of quantum correlations with applications in quantum sensing and simulation. While here we focused on the limit of Heisenberg in-plane interactions that favor spin alignment within layers, and thus homogeneous excitations predominantly in the fully symmetric manifold within the layers, by using a more general type of intralayer spin Hamiltonians enriched by the anisotropic nature of the dipolar interactions, one should be able to generate spatially dependent and anisotropic excitations featuring rich nonequilibrium universal behaviors [81]. Furthermore, the use of time-reversal protocols should enable measurements of out-of-time-order correlations [82] to better quantify correlation growth, or to realize SU(1,1) interferometry [38]. The phenomenology discussed here might be even further enriched utilizing dipoles with a larger internal state space, e.g., multiple rotational states of molecules or larger spin magnetic atoms.

We acknowledge careful review of this manuscript and useful comments from Calder Miller, Lindsay Sonderhouse, and Luis Santos. The work is supported by the AFOSR MURI, by the DARPA DRINQs Grant, the ARO single investigator Award W911NF-19-1-0210, the NSF JILA-PFC PHY-1734006 Grants, NSF QLCI-2016244 Grants, by the DOE Quantum Systems Accelerator (QSA) Grant and by NIST.

[1] C. Gross and W. S. Bakr, Quantum gas microscopy for single atom and spin detection, Nat. Phys. **17**, 1316 (2021).
[2] A. M. Kaufman and K.-K. Ni, Quantum science with optical tweezer arrays of ultracold atoms and molecules, Nat. Phys. **17**, 1324 (2021).
[3] C. J. Vale and M. Zwierlein, Spectroscopic probes of quantum gases, Nat. Phys. **17**, 1305 (2021).
[4] I. Bloch, Ultracold quantum gases in optical lattices, Nat. Phys. **1**, 23 (2005).
[5] I. Bloch, J. Dalibard, and W. Zwerger, Many-body physics with ultracold gases, Rev. Mod. Phys. **80**, 885 (2008).
[6] J. L. Bohn, A. M. Rey, and J. Ye, Cold molecules: Progress in quantum engineering of chemistry and quantum matter, Science **357**, 1002 (2017).
[7] S. A. Moses, J. P. Covey, M. T. Miecnikowski, D. S. Jin, and J. Ye, New frontiers for quantum gases of polar molecules, Nat. Phys. **13**, 13 (2016).
[8] M. A. Baranov, M. Dalmonte, G. Pupillo, and P. Zoller, Condensed matter theory of dipolar quantum gases, Chem. Rev. **112**, 5012 (2012).
[9] A. Browaeys and T. Lahaye, Many-body physics with individually controlled Rydberg atoms, Nat. Phys. **16**, 132 (2020).
[10] M. Morgado and S. Whitlock, Quantum simulation and computing with Rydberg-interacting qubits, AVS Quantum Sci. **3**, 023501 (2021).
[11] T. Lahaye, C. Menotti, L. Santos, M. Lewenstein, and T. Pfau, The physics of dipolar bosonic quantum gases, Rep. Prog. Phys. **72**, 126401 (2009).
[12] L. Chomaz, I. Ferrier-Barbut, F. Ferlaino, B. Laburthe-Tolra, B. L. Lev, and T. Pfau, Dipolar physics: A review of experiments with magnetic quantum gases, Rep. Prog. Phys. **86**, 026401 (2023).
[13] N. Defenu, T. Donner, T. Macrì, G. Pagano, S. Ruffo, and A. Trombettoni, Long-range interacting quantum systems, arXiv:2109.01063.
[14] F. Mivehvar, F. Piazza, T. Donner, and H. Ritsch, Cavity QED with quantum gases: New paradigms in many-body physics, Adv. Phys. **70**, 1 (2021).
[15] M. A. Norcia, R. J. Lewis-Swan, J. R. K. Cline, B. Zhu, A. M. Rey, and J. K. Thompson, Cavity-mediated collective spin-exchange interactions in a strontium superradiant laser, Science **361**, 259 (2018).
[16] S. J. Masson, M. D. Barrett, and S. Parkins, Cavity QED Engineering of Spin Dynamics and Squeezing in a Spinor Gas, Phys. Rev. Lett. **119**, 213601 (2017).
[17] E. J. Davis, G. Bentsen, L. Homeier, T. Li, and M. H. Schleier-Smith, Photon-Mediated Spin-Exchange Dynamics of Spin-1 Atoms, Phys. Rev. Lett. **122**, 010405 (2019).
[18] R. Blatt and C. F. Roos, Quantum simulations with trapped ions, Nat. Phys. **8**, 277 (2012).
[19] C. Monroe, W. C. Campbell, L.-M. Duan, Z.-X. Gong, A. V. Gorshkov, P. W. Hess, R. Islam, K. Kim, N. M. Linke, G. Pagano, P. Richerme, C. Senko, and N. Y. Yao, Programmable quantum simulations of spin systems with trapped ions, Rev. Mod. Phys. **93**, 025001 (2021).
[20] I. Bloch, J. Dalibard, and S. Nascimbène, Quantum simulations with ultracold quantum gases, Nat. Phys. **8**, 267 (2012).
[21] C. Gross and I. Bloch, Quantum simulations with ultracold atoms in optical lattices, Science **357**, 995 (2017).
[22] A. J. Daley, I. Bloch, C. Kokail, S. Flannigan, N. Pearson, M. Troyer, and P. Zoller, Practical quantum advantage in quantum simulation, Nature (London) **607**, 667 (2022).
[23] L. Pezzè, A. Smerzi, M. K. Oberthaler, R. Schmied, and P. Treutlein, Quantum metrology with nonclassical states of atomic ensembles, Rev. Mod. Phys. **90**, 035005 (2018).

[24] H.-J. Briegel, T. Calarco, D. Jaksch, J. I. Cirac, and P. Zoller, Quantum computing with neutral atoms, J. Mod. Opt. **47**, 415 (2000).

[25] D. S. Weiss and M. Saffman, Quantum computing with neutral atoms, Phys. Today **70**, No. 7, 44 (2017).

[26] L. Henriet, L. Beguin, A. Signoles, T. Lahaye, A. Browaeys, G.-O. Reymond, and C. Jurczak, Quantum computing with neutral atoms, Quantum **4**, 327 (2020).

[27] R. J. Lewis-Swan, A. Safavi-Naini, A. M. Kaufman, and A. M. Rey, Dynamics of quantum information, Nat. Rev. Phys. **1**, 627 (2019).

[28] A. Einstein, B. Podolsky, and N. Rosen, Can quantum-mechanical description of physical reality be considered complete?, Phys. Rev. **47**, 777 (1935).

[29] M. D. Reid, P. D. Drummond, W. P. Bowen, E. G. Cavalcanti, P. K. Lam, H. A. Bachor, U. L. Andersen, and G. Leuchs, Colloquium: The Einstein-Podolsky-Rosen paradox: From concepts to applications, Rev. Mod. Phys. **81**, 1727 (2009).

[30] G. Agarwal, *Quantum Optics* (Cambridge University Press, Cambridge, England, 2013), 10.1017/cbo9781139035170.

[31] C. M. Caves and B. L. Schumaker, New formalism for two-photon quantum optics. I. Quadrature phases and squeezed states, Phys. Rev. A **31**, 3068 (1985).

[32] B. L. Schumaker and C. M. Caves, New formalism for two-photon quantum optics. II. Mathematical foundation and compact notation, Phys. Rev. A **31**, 3093 (1985).

[33] P. Hauke, D. Marcos, M. Dalmonte, and P. Zoller, Quantum Simulation of a Lattice Schwinger Model in a Chain of Trapped Ions, Phys. Rev. X **3**, 041018 (2013).

[34] V. Kasper, F. Hebenstreit, M. Oberthaler, and J. Berges, Schwinger pair production with ultracold atoms, Phys. Lett. B **760**, 742 (2016).

[35] J. Hu, L. Feng, Z. Zhang, and C. Chin, Quantum simulation of Unruh radiation, Nat. Phys. **15**, 785 (2019).

[36] C. Gross, H. Strobel, E. Nicklas, T. Zibold, N. Bar-Gill, G. Kurizki, and M. K. Oberthaler, Atomic homodyne detection of continuous-variable entangled twin-atom states, Nature (London) **480**, 219 (2011).

[37] B. Lücke, M. Scherer, J. Kruse, L. Pezzé, F. Deuretzbacher, P. Hyllus, O. Topic, J. Peise, W. Ertmer, J. Arlt, L. Santos, A. Smerzi, and C. Klempt, Twin matter waves for interferometry beyond the classical limit, Science **334**, 773 (2011).

[38] D. Linnemann, H. Strobel, W. Muessel, J. Schulz, R. J. Lewis-Swan, K. V. Kheruntsyan, and M. K. Oberthaler, Quantum-Enhanced Sensing Based on Time Reversal of Nonlinear Dynamics, Phys. Rev. Lett. **117**, 013001 (2016).

[39] A. Qu, B. Evrard, J. Dalibard, and F. Gerbier, Probing Spin Correlations in a Bose-Einstein Condensate Near the Single-Atom Level, Phys. Rev. Lett. **125**, 033401 (2020).

[40] S. Chapman, J. Eisert, L. Hackl, M. P. Heller, R. Jefferson, H. Marrochio, and R. C. Myers, Complexity and entanglement for thermofield double states, SciPost Phys. **6**, 034 (2019).

[41] D. Zhu, S. Johri, N. M. Linke, K. A. Landsman, C. H. Alderete, N. H. Nguyen, A. Y. Matsuura, T. H. Hsieh, and C. Monroe, Generation of thermofield double states and critical ground states with a quantum computer, Proc. Natl. Acad. Sci. U.S.A. **117**, 25402 (2020).

[42] L. Chomaz, I. Ferrier-Barbut, F. Ferlaino, B. Laburthe-Tolra, B. L. Lev, and T. Pfau, Dipolar physics: A review of experiments with magnetic quantum gases, Rep. Prog. Phys. **86**, 026401 (2023).

[43] A. Browaeys and T. Lahaye, Many-body physics with individually controlled Rydberg atoms, Nat. Phys. **16**, 132 (2020).

[44] M. Saffman, T. G. Walker, and K. Mølmer, Quantum information with Rydberg atoms, Rev. Mod. Phys. **82**, 2313 (2010).

[45] P. Scholl, H. J. Williams, G. Bornet, F. Wallner, D. Barredo, L. Henriet, A. Signoles, C. Hainaut, T. Franz, S. Geier, A. Tebben, A. Salzinger, G. Zürn, T. Lahaye, M. Weidemüller, and A. Browaeys, Microwave engineering of programmable *xxz* Hamiltonians in arrays of Rydberg atoms, PRX Quantum **3**, 020303 (2022).

[46] S. Geier, N. Thaicharoen, C. Hainaut, T. Franz, A. Salzinger, A. Tebben, D. Grimshandl, G. Zürn, and M. Weidemüller, Floquet Hamiltonian engineering of an isolated many-body spin system, Science **374**, 1149 (2021).

[47] L. Christakis, J. S. Rosenberg, R. Raj, S. Chi, A. Morningstar, D. A. Huse, Z. Z. Yan, and W. S. Bakr, Probing site-resolved correlations in a spin system of ultracold molecules, Nature (London) **614**, 64 (2023).

[48] W. G. Tobias, K. Matsuda, J.-R. Li, C. Miller, A. N. Carroll, T. Bilitewski, A. M. Rey, and J. Ye, Reactions between layer-resolved molecules mediated by dipolar spin exchange, Science **375**, 1299 (2022).

[49] C. M. Holland, Y. Lu, and L. W. Cheuk, On-demand entanglement of molecules in a reconfigurable optical tweezer array, arXiv:2210.06309.

[50] K. Hammerer, A. S. Sørensen, and E. S. Polzik, Quantum interface between light and atomic ensembles, Rev. Mod. Phys. **82**, 1041 (2010).

[51] S. J. Freedman and J. F. Clauser, Experimental Test of Local Hidden-Variable Theories, Phys. Rev. Lett. **28**, 938 (1972).

[52] A. Aspect, P. Grangier, and G. Roger, Experimental Tests of Realistic Local Theories via Bell's Theorem, Phys. Rev. Lett. **47**, 460 (1981).

[53] Z. Y. Ou, S. F. Pereira, H. J. Kimble, and K. C. Peng, Realization of the Einstein-Podolsky-Rosen Paradox for Continuous Variables, Phys. Rev. Lett. **68**, 3663 (1992).

[54] B. Julsgaard, A. Kozhekin, and E. S. Polzik, Experimental long-lived entanglement of two macroscopic objects, Nature (London) **413**, 400 (2001).

[55] N. J. Cerf, G. Leuchs, and E. S. Polzik, *Quantum Information with Continuous Variables of Atoms and Light* (World Scientific, Singapore, 2007).

[56] M. Fadel, T. Zibold, B. Décamps, and P. Treutlein, Spatial entanglement patterns and Einstein-Podolsky-Rosen steering in a Bose-Einstein condensate, Science **360**, 409 (2017).

[57] P. Kunkel, M. Prüfer, H. Strobel, D. Linnemann, A. Frölian, T. Gasenzer, M. Gärttner, and M. K. Oberthaler, Spatially distributed multipartite entanglement enables EPR steering of atomic clouds, Science **360**, 413 (2018).

[58] L. J. Stephenson, D. P. Nadlinger, B. C. Nichol, S. An, P. Drmota, T. G. Ballance, K. Thirumalai, J. F. Goodwin, D. M. Lucas, and C. J. Ballance, High-Rate, High-Fidelity Entanglement of Qubits Across an Elementary Quantum Network, Phys. Rev. Lett. **124**, 110501 (2020).

[59] B. C. Nichol, R. Srinivas, D. P. Nadlinger, P. Drmota, D. Main, G. Araneda, C. J. Ballance, and D. M. Lucas, An elementary quantum network of entangled optical atomic clocks, Nature (London) **609**, 689 (2022).
[60] Y. Wan, D. Kienzler, S. D. Erickson, K. H. Mayer, T. R. Tan, J. J. Wu, H. M. Vasconcelos, S. Glancy, E. Knill, D. J. Wineland, A. C. Wilson, and D. Leibfried, Quantum gate teleportation between separated qubits in a trapped-ion processor, Science **364**, 875 (2019).
[61] D. Lago-Rivera, S. Grandi, J. V. Rakonjac, A. Seri, and H. de Riedmatten, Telecom-heralded entanglement between multimode solid-state quantum memories, Nature (London) **594**, 37 (2021).
[62] E. S. Polzik and J. Ye, Entanglement and spin squeezing in a network of distant optical lattice clocks, Phys. Rev. A **93**, 021404(R) (2016).
[63] A. Y. Kitaev, Unpaired Majorana fermions in quantum wires, Phys. Usp. **44**, 131 (2001).
[64] A. McDonald, T. Pereg-Barnea, and A. A. Clerk, Phase-Dependent Chiral Transport and Effective non-Hermitian Dynamics in a Bosonic Kitaev-Majorana Chain, Phys. Rev. X **8**, 041031 (2018).
[65] A. M. Rey, L. Jiang, M. Fleischhauer, E. Demler, and M. D. Lukin, Many-body protected entanglement generation in interacting spin systems, Phys. Rev. A **77**, 052305 (2008).
[66] P. Cappellaro and M. D. Lukin, Quantum correlation in disordered spin systems: Applications to magnetic sensing, Phys. Rev. A **80**, 032311 (2009).
[67] M. P. Kwasigroch and N. R. Cooper, Bose-Einstein condensation and many-body localization of rotational excitations of polar molecules following a microwave pulse, Phys. Rev. A **90**, 021605(R) (2014).
[68] E. J. Davis, A. Periwal, E. S. Cooper, G. Bentsen, S. J. Evered, K. VanKirk, and M. H. Schleier-Smith, Protecting Spin Coherence in a Tunable Heisenberg Model, Phys. Rev. Lett. **125**, 060402 (2020).
[69] M. A. Perlin, C. Qu, and A. M. Rey, Spin Squeezing with Short-Range Spin-Exchange Interactions, Phys. Rev. Lett. **125**, 223401 (2020).
[70] J. Schachenmayer, A. Pikovski, and A. M. Rey, Many-Body Quantum Spin Dynamics with Monte Carlo Trajectories on a Discrete Phase Space, Phys. Rev. X **5**, 011022 (2015).
[71] B. Zhu, A. M. Rey, and J. Schachenmayer, A generalized phase space approach for solving quantum spin dynamics, New J. Phys. **21**, 082001 (2019).
[72] B. Sundar, K. C. Wang, and K. R. A. Hazzard, Analysis of continuous and discrete Wigner approximations for spin dynamics, Phys. Rev. A **99**, 043627 (2019).
[73] J. Wurtz, A. Polkovnikov, and D. Sels, Cluster truncated Wigner approximation in strongly interacting systems, Ann. Phys. (Amsterdam) **395**, 341 (2018).
[74] M. Kolodrubetz, D. Sels, P. Mehta, and A. Polkovnikov, Geometry and non-adiabatic response in quantum and classical systems, Phys. Rep. **697**, 1 (2017).
[75] B. Berg, L. I. Plimak, A. Polkovnikov, M. K. Olsen, M. Fleischhauer, and W. P. Schleich, Commuting Heisenberg operators as the quantum response problem: Time-normal averages in the truncated Wigner representation, Phys. Rev. A **80**, 033624 (2009).
[76] T. Holstein and H. Primakoff, Field dependence of the intrinsic domain magnetization of a ferromagnet, Phys. Rev. **58**, 1098 (1940).
[77] See Supplemental Material at http://link.aps.org/supplemental/10.1103/PhysRevLett.131.053001, which also contains Refs. [70–75,78–80], for additional details on the excitations beyond the collective limit, limits of the second order Holstein-Primakof transformation, and the effects of decoherence and finite filling fraction, the frame transformation for spiral states, the exact solution of the bosonic Kitaev model, and the comparison of the analytical results of the bosonic Kitaev model with the dipolar spin dynamics.
[78] B. Sundar, D. Barberena, A. P. Orioli, A. Chu, J. K. Thompson, A. M. Rey, and R. J. Lewis-Swan, Bosonic Pair Production and Squeezing for Optical Phase Measurements in Long-Lived Dipoles Coupled to a Cavity, Phys. Rev. Lett. **130**, 113202 (2023).
[79] F. J. dos Santos, M. dos Santos Dias, F. S. M. Guimarães, J. Bouaziz, and S. Lounis, Spin-resolved inelastic electron scattering by spin waves in noncollinear magnets, Phys. Rev. B **97**, 024431 (2018).
[80] T. Bilitewski, G. A. Domínguez-Castro, D. Wellnitz, A. M. Rey, and L. Santos, Momentum-selective pair creation of spin excitations in dipolar bilayers, arXiv:2302.09059.
[81] J. F. Rodriguez-Nieva, A. P. Orioli, and J. Marino, Far-from-equilibrium universality in the two-dimensional Heisenberg model, Proc. Natl. Acad. Sci. U.S.A. **119**, e2122599119 (2022).
[82] M. Gärttner, J. G. Bohnet, A. Safavi-Naini, M. L. Wall, J. J. Bollinger, and A. M. Rey, Measuring out-of-time-order correlations and multiple quantum spectra in a trapped-ion quantum magnet, Nat. Phys. **13**, 781 (2017).